Functional Effects of Nanoparticle Exposure on Calu-3 Airway Epithelial Cells

4 authors, including:

Amiraj Banga
Indiana University-Purdue University Indianapolis
3 PUBLICATIONS   **50** CITATIONS

SEE PROFILE

Frank A Witzmann
Indiana University School of Medicine
241 PUBLICATIONS   **4,182** CITATIONS

SEE PROFILE

Cellular Physiology and Biochemistry

Functional Effects of Nanoparticle Exposure on Calu-3 Airway Epithelial Cells

Amiraj Banga[1], Frank A. Witzmann[2], Horia I. Petrache[3], Bonnie L. Blazer-Yost[1,2]

[1]Department of Biology, Indiana University Purdue University Indianapolis, [2]Department of Cellular & Integrative Physiology, Indiana University School of Medicine Indianapolis, [3]Department of Physics, Indiana University Purdue University Indianapolis

Abstract
High concentrations of manufactured carbon nanoparticles (CNP) are known to cause oxidative stress, inflammatory responses and granuloma formation in respiratory epithelia. To examine the effects of lower, more physiologically relevant concentrations, the human airway epithelial cell line, Calu-3, was used to evaluate potential alterations in transepithelial permeability and cellular function of airway epithelia after exposure to environmentally realistic concentrations of carbon nanoparticles. Three common carbon nanoparticles, fullerenes, single- and multi-wall carbon nanotubes (SWCNT, MWCNT) were used in these experiments. Electro-physiological measurements were performed to assay transepithelial electrical resistance (TEER) and epinephrine-stimulated chloride (Cl⁻) ion secretion of epithelial cell monolayers that had been exposed to nanoparticles for three different times (1 h, 24 h and 48 h) and over a 7 log unit range of concentrations.

Fullerenes did not have any effect on the TEER or stimulated ion transport. However, the carbon nanotubes (CNT) significantly decreased TEER and inhibited epinephrine-stimulated Cl⁻ secretion. The changes were time dependent and at more chronic exposures caused functional effects which were evident at concentrations substantially lower than have been previously examined. The functional changes manifested in response to physiologically relevant exposures would inhibit mucociliary clearance mechanisms and compromise the barrier function of airway epithelia.

Copyright © 2012 S. Karger AG, Basel

Introduction

Nanotechnology, the creation and manipulation of structures and systems at a nanoscale level (<100 nm), produces materials with significantly altered fundamental properties. These properties include unique surface area/volume ratios, refractive indices, hydrophobicity, biological

Bonnie L. Blazer-Yost
Indiana University - Purdue University
Biology Department, SL 358 - 723 West Michigan Street
Indianapolis, IN 46202 (USA)
Tel. +1 317-278-1145, Fax +1 317-274-2846, E-Mail bblazer@iupui.edu

and chemical reactivity. Such novel properties have been put to various uses by industries such as electronic, pharmaceutical, biomedical, automotive, engineering, agricultural, cosmetic and aerospace. Consequently, literally tons of nanoparticles are being produced in industrialized nations. With nanotechnology being a focused area of scientific and industrial growth in the last few decades, concerns have arisen regarding the potential biological effects of nanoscale materials. These effects remain poorly understood, especially with regard to occupational and environmental hazards [1-11]. Populations exposed to increasing levels of nanomaterials include not only workers exposed during the production, recycling and disposal, but also to the general population that uses commercially available nanomaterial-containing products and also has contact via environmental contamination.

The unique physico-chemical properties of these nanoscale products cause them to interact with cellular systems in an unknown and undefined manner. Potential injurious cellular effects of these particles have been reviewed by various authors [1-11]. Demonstrated effects include oxidative stress, inflammatory cytokine production, fibrosis, DNA mutation, membrane damage, granuloma formation and even cell death [8-10]. Although the nanotechnology industry holds great promise in the future, its darker side has to be explored to obtain the maximum benefits from this industry in a safe manner.

Carbon based nanoparticles are one group of widely produced nanomaterials. These include fullerenes and nanotubes (single-wall carbon nanotubes (SWCNT) and multi-wall carbon nanotubes (MWCNT)). Fullerenes, or Buckyballs, are quite stable structures composed of 60 carbon atoms with an average diameter of 0.72 nm. Carbon nanotubes (CNTs) are graphite sheets rolled to form seamless tubes or cylinders. Whereas SWCNT consist of a single layer with diameters of a few nm, MWCNT are larger and consist of many single-walled tubes stacked one inside the other with total diameters reaching up to 100 nm. CNTs are found in various lengths in the μm range. Because of their nano sizes, fibrous shapes and carbon base, CNTs are expected to behave differently than the large sized particles. They are potentially toxic like other small fibers (asbestos and silica) and biopersistent because of their stability [11].

One primary route of CNP uptake in the body is through inspiration of airborne nanoparticles where they can cause airway and lung disease [12-15]. In addition, following inhalation, ultrafine carbon particles can enter the circulatory system and thereby have access to multiple organs including the brain [16, 17]. MWCNTs have been shown to reach the subpleural tissue in mice with a single inhalation dose of 30 mg/m^3 for 6 h [18]. In the circulatory system per se, SWCNTs can have prothrombotic effects *in vivo* and demonstrate platelet activation *in vitro* [19]. A stable C_{60} suspension has been shown to produce genotoxicity as a result of DNA damage in human lymphocytes [10].

One of the respiratory cell lines commonly used for tracheobronchial epithelial cell studies is Calu-3. Although it is adenocarcinoma in origin, it is one of the few cell lines that form tight junctions *in vitro* and demonstrates the characteristics of differentiated, functional human airway epithelia [20, 21]. The current studies utilize this well-characterized model to study the effects of unpurified, as manufactured, nanoparticles that are most likely to be found as environmental and occupational pollutants.

Materials and Methods

Materials

Dulbecco's minimal essential media (DMEM/F-12), Glutamax, penicillin, streptomycin, sodium pyruvate (100 X), non-essential amino-acids (100 X) were purchased from Invitrogen (Carlsbad, CA). Fetal bovine serum (FBS) was from Gemini Bioproducts, (West Sacramento, CA). Cell culture flasks and transwell cell culture plates (24 mm inserts, polycarbonate, 0.4 μm pore size) were obtained from Costar-Corning (Acton, MA). Other cell culture reagents including 10 X trypsin-EDTA solution (0.5 %) and Hanks balanced salt solution (HBSS) were obtained from Mediatech, Inc, (Herndon, VA.). CNPs were purchased from SES Research (Houston, TX) and used with no further purification.

Cell Culture

The Calu-3 (ATCC no. HTB-55) cell line was purchased from American Type Culture Collection (Manassas, VA) at passage 19. Cells were grown in humidified atmosphere of 5 % CO_2-95 % air at 37°C. The culture media were comprised of DMEM/F-12 (1:1), 15 % FBS, 2.40 mg/L $NaHCO_3$, 100 U/L penicillin, 100 mg/L streptomycin, 0.5 mM non-essential amino acids, 0.5 mM sodium pyruvate and 1 mM Glutamax.

The medium was replaced thrice weekly and cells were passaged weekly at a split ratio of 1:4. For electrophysiology, the cells were seeded directly on the permeable filters of the transwell cell culture plates with media on the apical and basolateral sides. Two days after inoculation, the media were removed from the apical side and replaced only on the basolateral side. This cell culture technique, called air interface culture (AIC), mimics the *in vivo* situation. The Calu-3 cells secrete a sufficient amount of fluid and mucus to remain hydrated. Cell monolayers were used on 14th day after being seeded on the transwells, the time at which the cells show a high resistance phenotype.

CNP Preparation

As reported by the manufacturer, fullerenes (C60) (#600-9980) are 99.95+ %, ultra-pure and vacuum oven-dried; SWCNT (#900-1301) (long) were purified single-wall nanotubes with an outer diameter <2 nm, lengths ranging from 5-15 μm, purity >90 % CNT (>50 % SWCNT), ash <2 % wt and amorphous carbon <5 % wt. MWCNT (# 900-1203) are purified multiwall nanotubes with an outer diameter of 40-60 nm, length ranging from 5-15 μm, >95 % nanotubes vs amorphous carbon (<2 %), and ash content <0.2 %.

Fullerenes, SWCNT, and MWCNT were prepared in FBS at a concentration of 5 mg/mL. Serum acts as a surfactant to disperse hydrophobic nanoparticles via destabilization of the aggregates by serum proteins [22]. At low nanomaterial concentrations, the presence of proteins has been reported to generate small agglomerates of particles with minimal size variations and improved the stability of the dispersions [23]. Samples were sonicated using a Branson Sonifier 450 at a duty cycle of 30 % and an output control of 3 for 20 seconds. Before sonication of each sample, the probe was cleaned with ethanol and coated for 10 seconds with serum. After sonication, the samples were autoclaved and diluted to a final concentration of nanoparticles in the cell culture media. Control FBS without nanoparticles was treated in an identical manner. Additional CNP-free FBS was added to a final concentration of 15 % FBS in culture media. Since Calu-3 cells require 15 % of FBS in the culture media, only 2 % of the total FBS was autoclaved with CNPs. The nanoparticles were added to the apical side of the cells after they developed a high resistance phenotype. Only 200 μl of CNP containing media was added to the apical side (5 cm^2) to maintain the AIC for the cells.

To examine the effect of short-term versus long term exposure, cells were treated with CNPs for 1, 24 or 48 hours. For the 1 and 24 hour time points, the CNPs were added only to the apical bathing medium to simulate a more acute exposure. For the 48 hour exposure, the CNPs were added to both the apical and basolateral bathing media.

The nanoparticle concentrations are shown as g/cm^2 to more accurately reflect the actual exposures. However all volumes were maintained in constant proportions so that the surface exposure can be converted into concentration per volume of media using the following formula: N g/cm^2 = 25N g/mL

Analysis of Particle Size and Zeta Potential of Nanoparticles in the Media

Cell culture media containing SWCNTs and MWCNTs were analyzed using a Nano Zetasizer ZS90 (Malvern Instruments, Worcestershire, UK). In this technique, particle size is the diameter of the sphere that diffuses at the same speed as the particle being measured. The Zetasizer system uses dynamic light scattering (DLS) to measure the Brownian motion of the particles in a sample.

Since smaller particles move rapidly in a liquid than larger particles, the position of two images of the sample separated by a short interval of time is used to determine the displacement of the particle and therefore its relative size. A minimal displacement with similar particle positions indicates that the particles in the sample are large whereas larger displacements with different particle positions indicate that the particles in the sample are small. Using this principle and the relationship between diffusion speed and size, the relative sizes can be determined. To mimic the normal cellular incubation conditions, the nanoparticle-containing media were prepared in the usual manner, incubated at 37°C and measured after 1, 24, 48 hours.

Zeta potential is a voltage that exists between the particle surface and the liquid in which it is dispersed and varies according to the distance from the particle surface. Zeta potential is measured using a combination of the measurement techniques: electrophoresis and laser doppler velocimetry, sometimes called laser doppler electrophoresis. This method measures how fast a particle moves in a liquid when an electrical field is applied – i.e. its velocity. Once the velocity of the particle is determined and the electrical field applied, one can, by using two other known constants of the sample – viscosity and dielectric constant, determine the zeta potential.

Electrophysiology

Electrophysiological techniques were used to measure transepithelial electric resistance (TEER) as well as to monitor changes in ion flux across the cellular monolayers in response to hormonal stimulation. Cells were grown to confluency on the transwell filters and exposed to CNPs for the times indicated in the figures. At the end of the incubation period, the filters were cut from the plastic inserts, mounted in a Ussing chamber that separates the apical (luminal) surface from basolateral (serosal). The Ussing chamber was connected to a DVC-1000 Voltage/Current Clamp (World Precision Instruments) with voltage and current electrodes on either side of the membrane. The spontaneous transepithelial potential difference was clamped to zero, and the resultant short-circuit current (SCC) was monitored continuously. SCC is a measure of net transepithelial ion flux. Typically, an increase in SCC is either due to cation absorption (apical to serosal transport) or anion secretion (serosal to apical transport). The cells were bathed in serum-free medium maintained at 37°C via water-jacketed buffer chambers on either side of the filter. Medium was circulated and kept at constant pH using a 5 % CO_2 / 95 % O_2 gas lift. A voltage pulse of 2 mV was applied every 200 s and the resulting current displacement was used to determine TEER by using Ohm's law. After the basal current stabilized (time=0), epinephrine (10^{-6} M) was added to the serosal bathing medium. Addition of NPPB, (100 μM) to the apical bathing medium was used to inhibit the Cl$^-$ secretion.

cAMP Assay

The Calu-3 cells were treated with media containing FBS-CNPs for 48 h, followed by stimulation with or without epinephrine (10^{-6} M) for 10 seconds. The cells were washed twice with HBSS at 37°C and incubated for 10 minutes with 1 % triton-X-100 in 0.1 M HCl at 37°C. Permeabilized cells were scraped from the underlying supports and lysates were centrifuged for 1 min at 14,000 x g to remove cellular debris. The cAMP assay was performed using Assay Designs Direct cyclic AMP EIA kit. (Ann Arbor, MI) following the manufacturer's instructions. Because nanotubes have the ability to adsorb a
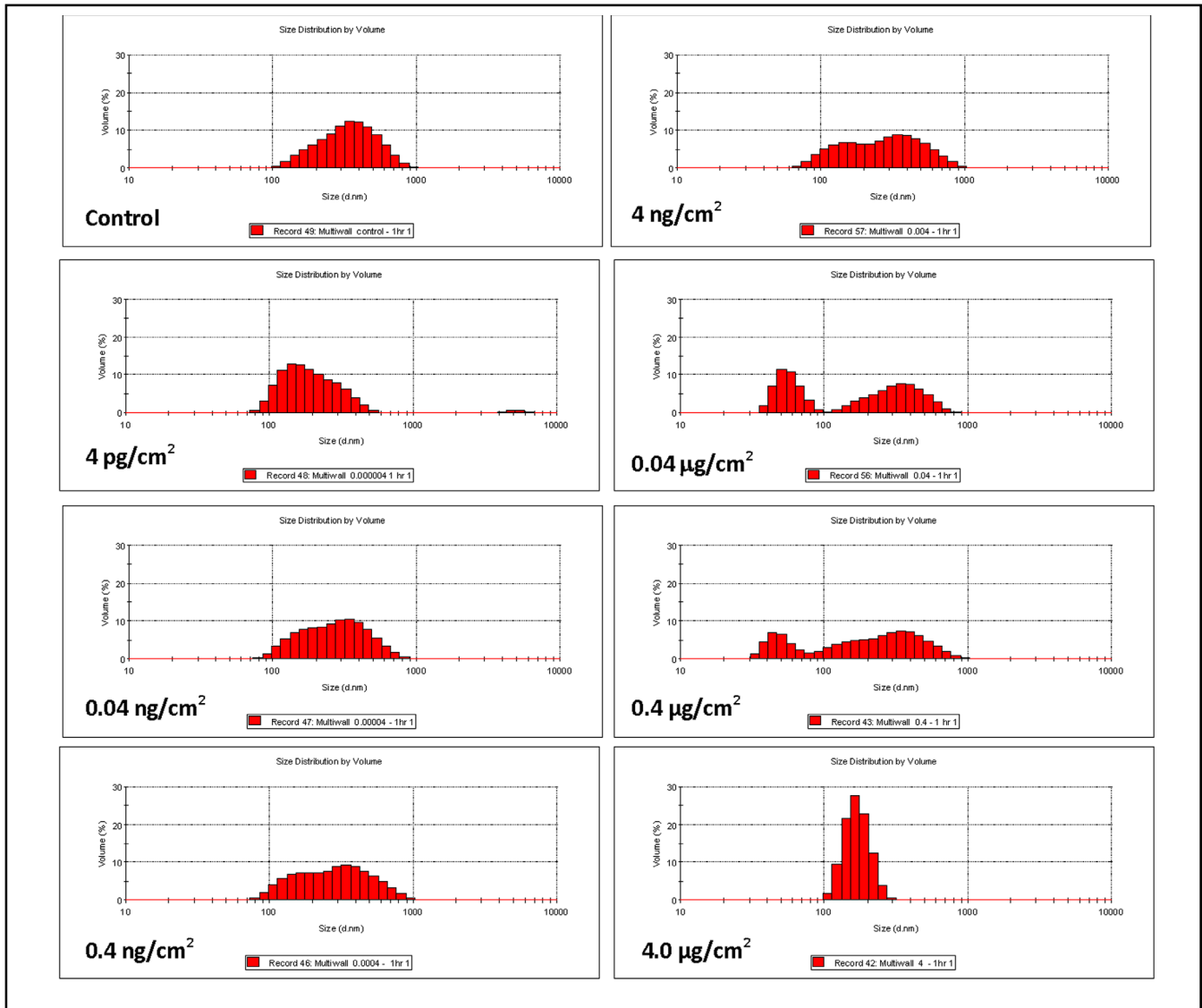
Fig. 1. Particle size measurement of MWCNTs - 1 h incubation. The culture media containing different concentrations (0, 4 µg/cm²-4 pg/cm²) of MWCNTs was prepared in a manner identical to the cell incubation media and incubated at 37 °C for 1 h. The particle sizes were measured by using Zetasizer nano ZS90. The graphs are the original printout from the Zetasizer. The graphs plot size (d.nm) on the x axis versus volume (%) on the Y axis. The top line on each Y axis is 30.

wide variety of small organic solutes, indicator dyes or their reduction products [24, 25] appropriate concentrations of nanoparticles were added to the controls at the time of the assay.

Cytokine Assay

Human inflammation ELISA strip for profiling cytokines (Signosis, Sunnyvale CA) was used to determine the relative amounts of eight cytokines: TNF-α (Tumor necrosis factor-alpha), IFNr (interferon regulator), G-CSF (granulocyte-colony stimulating factor), GM-CSF (granulocyte macrophage-colony stimulating factor), IL-1a (interleukin-1a), IL-8 (interleukin-8), IP-10 (interferon inducible protein 10), and RANTES (regulated on activation, normal T expressed and secreted) in the

apical and basolateral media from Calu-3 cell cultures. The assay was done in triplicate according to the given protocol. Due to their large surface area, nanoparticles have the ability to adsorb a wide variety of small organic solutes, indicator dyes or their reduction products [24, 25]. Since this is a colorimetric assay, therefore, we carried out controls for this assay with addition of nanoparticles at the time of the assay.

Statistical Analyses

Line and bar graphs have been generated using SigmaPlot 8.0 software. The points in the line graphs and bars in the bar graphs represent means ±SEM. Students t-test was used to determine statistical differences ($p < 0.05$).
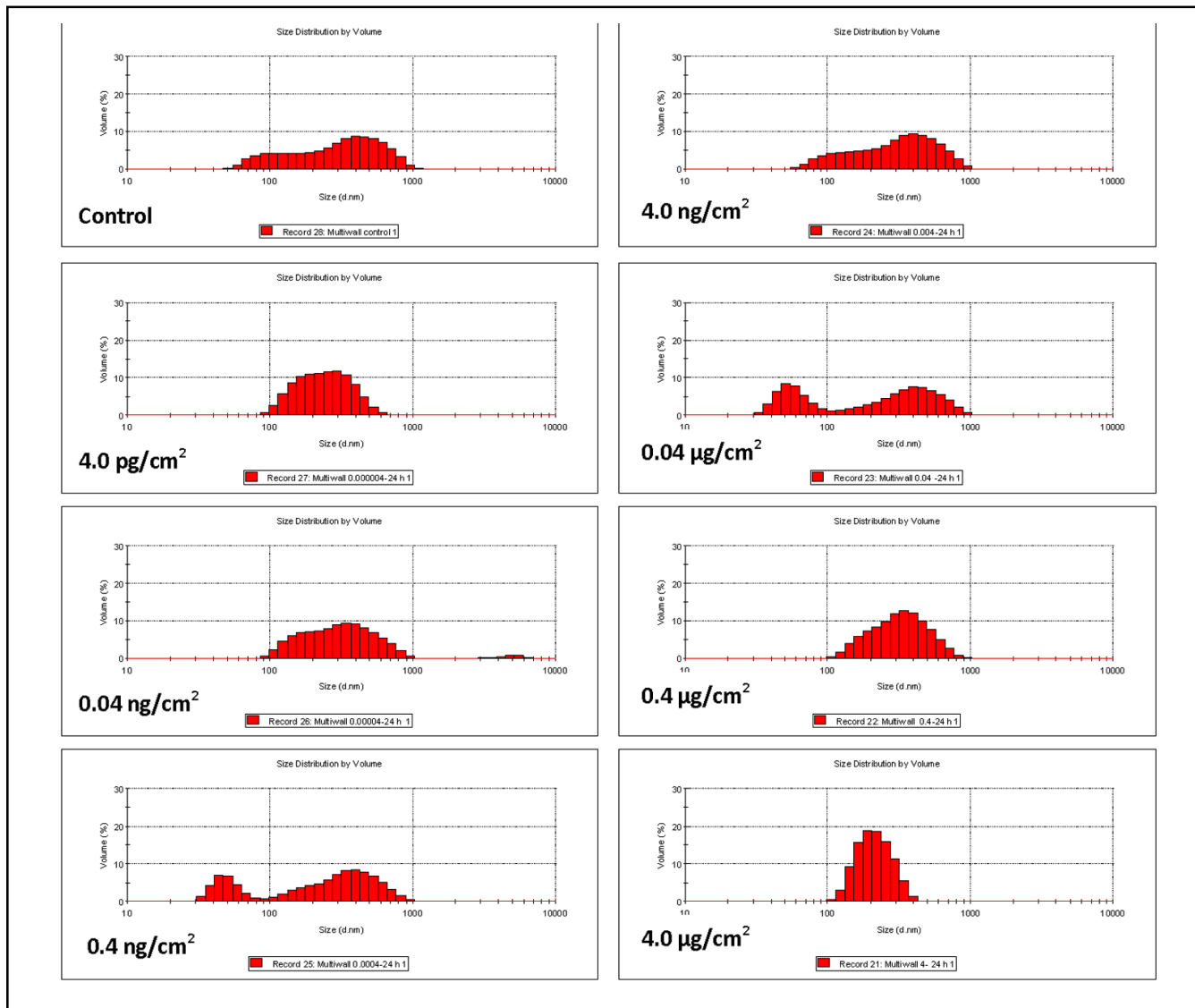
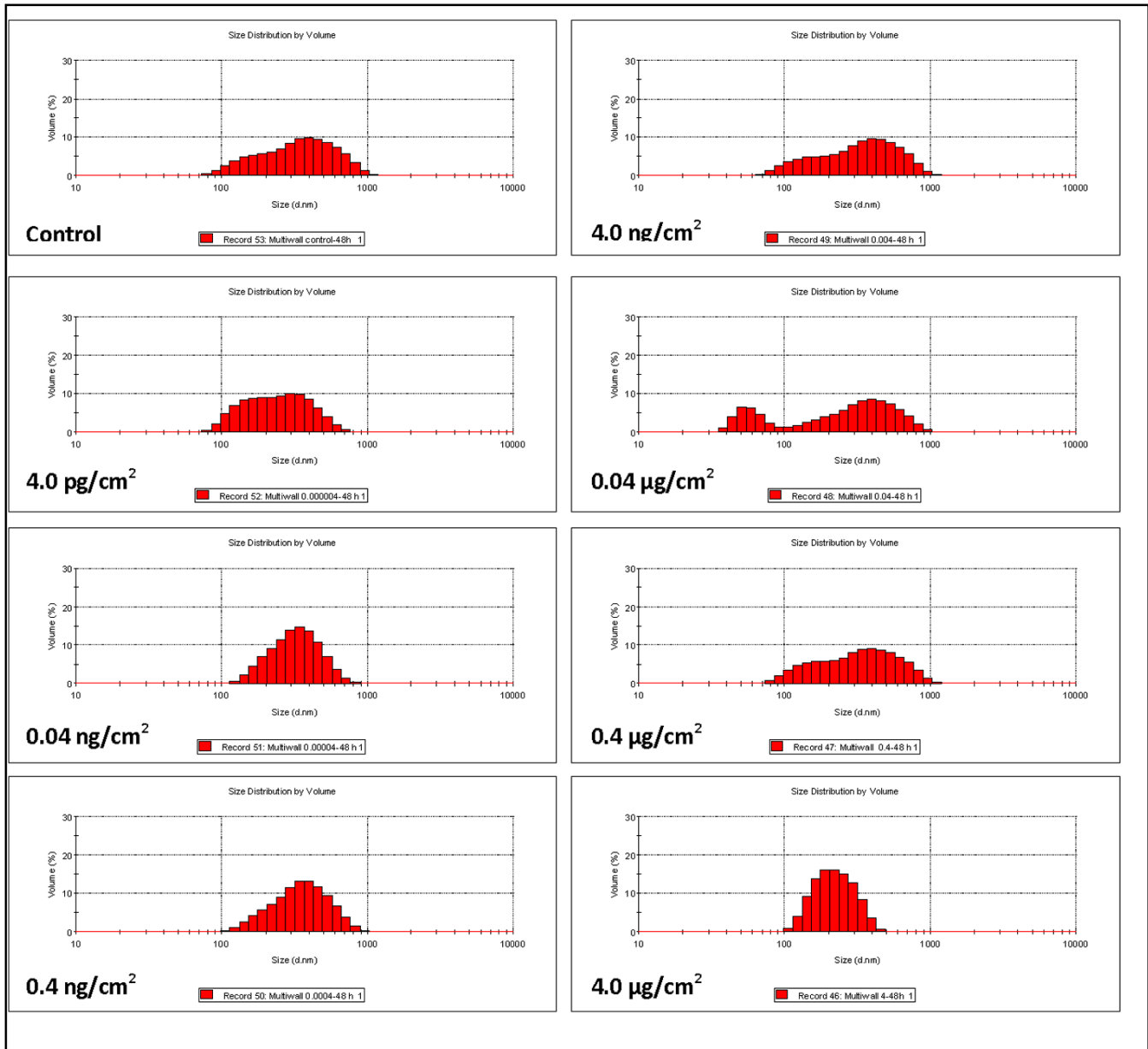**Fig. 2.** Particle size measurement of MWCNTs - 24 h incubation. The culture media containing different concentrations (0, 4 µg/cm²-4 pg/cm²) of MWCNTs was prepared in a manner identical to the cell incubation media and incubated at 37 °C for 24 h. The particle sizes were measured by using Zetasizer nano ZS90. The graphs are the original printout from the Zetasizer. The graphs plot size (d.nm) on the x axis versus volume (%) on the Y axis. The top line on each Y axis is 30.

Results

The nanomaterials used in these studies were partially characterized previously. Elemental analysis by energy dispersion X-ray spectroscopy of the three types of particles indicate that the fullerenes are virtually free of contaminating metals while the carbon nanotubes have low but measureable levels of iron (0.4 %), nickel (0.3-1 %) and/or cobalt (0.2-4.3 %) which are likely contaminants from the manufacturing process [26]. Scanning electron microscopy of SWCNT and MWCNT indicated that these materials are relatively free of amorphous carbon [26].

The relative particle size measurements of different concentrations (4 pg/cm²- 4 µg/cm²) of SWCNTs and MWCNTs in the Calu-3 culture media are shown in Figs. 1-6. Controls were prepared in culture media with the same serum as the nanoparticle solutions therefore the predominate measured particles in the control are due to serum proteins.

Measurements of particle sizes in culture media containing MWCNTs and SWCNTS are shown in Figs. 1-3 and Figs. 4-6, respectively. For each kind of CNT, measurements were performed at 1h, 24h, and 48h after incubation. In all 6 figures, the culture media presents a broad distribution of sizes between 100 and 1000 nm (0.1
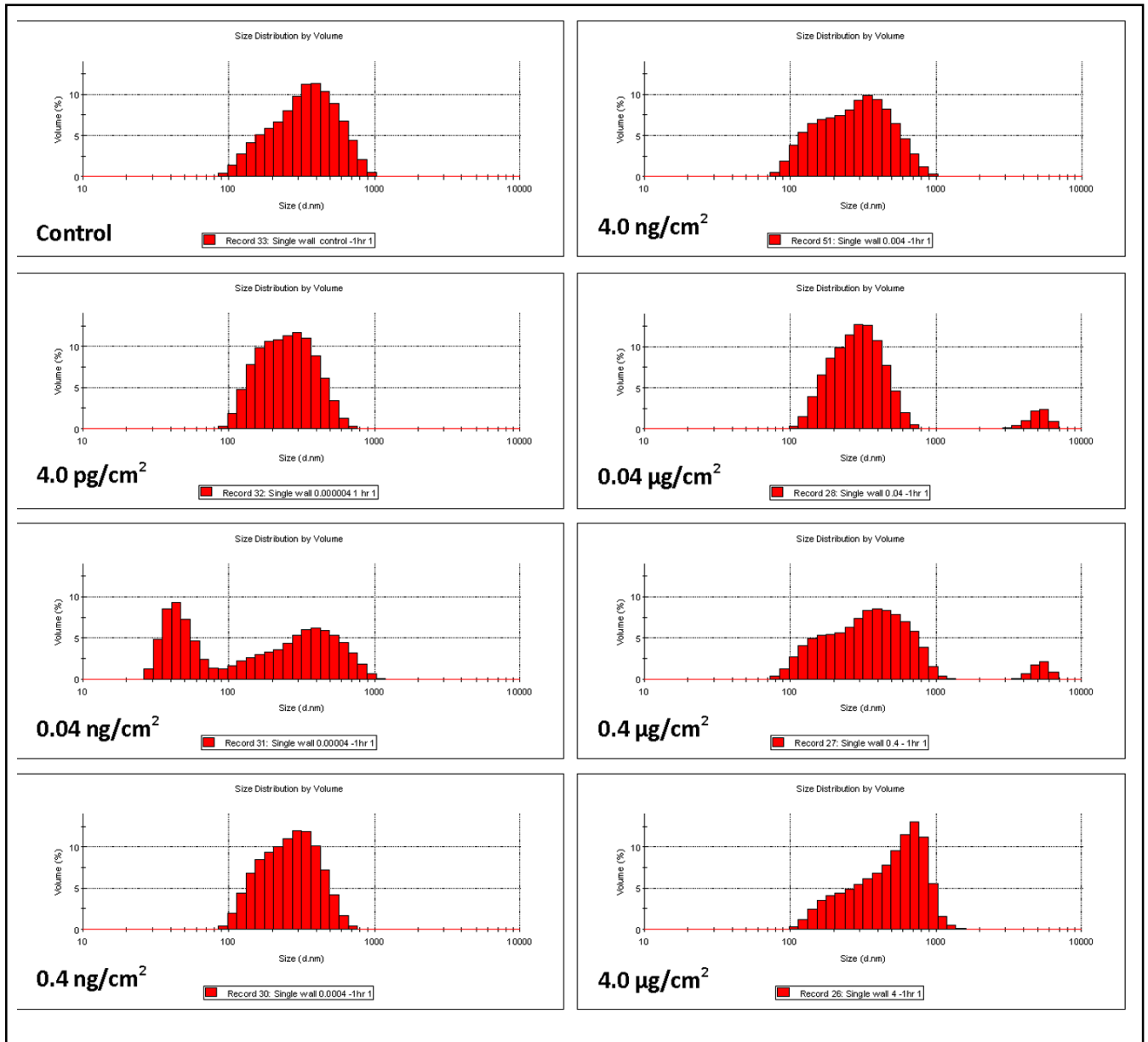
Fig. 3. Particle size measurement of MWCNTs - 48 h incubation. The culture media containing different concentrations (0, 4 µg/cm^2-4 pg/cm^2) of MWCNTs was prepared in a manner identical to the cell incubation media and incubated at 37 °C for 48 h. The particle sizes were measured by using Zetasizer nano ZS90. The graphs are the original printout from the Zetasizer. The graphs plot size (d.nm) on the x axis versus volume (%) on the Y axis. The top line on each Y axis is 30.

to 1 micron) with a peak around 400 nm, except for the control measurement in Figs. 2, 3 at 24h and 48h for which the culture media presents a shoulder at 100 nm.

When CNT particles are added to the media, modifications in the size distribution are observed. In the case of MWCNTs (Figs.1-3), a general shift toward smaller sizes is observed above 0.4 ng/cm^2 concentrations. As CNT concentration increases, a secondary peak in the distribution arises corresponding to particles around and below 100 nm. At the highest concentration measured

(4 µg/cm^2) a narrow distribution is seen between 100 and 300 nm which becomes broader with time. (Some variations with time are also seen for smaller concentrations.) These results show that CNT nanoparticles interact with molecules in the culture media to form new aggregates. Note that any particles or aggregates that are either smaller than 10 nm or larger than 10 microns go undetected by the instrument.

Changes in size distribution also occur with addition of SWCNT (Figs. 4-6) although the trends appear more

Fig. 4. Particle size measurement of SWCNTs - 1 h incubation. The culture media containing different concentrations (0, 4 µg/cm²-4 pg/cm²) of SWCNTs was prepared in a manner identical to the cell incubation media and incubated at 37 °C for 1 h. The particle sizes were measured by using Zetasizer nano ZS90. The graphs are the original printout from the Zetasizer. The graphs plot size (d.nm) on the x axis versus volume (%) on the Y axis. The top line on each Y axis is 10.

complicated than in the case of MWCNTs. A secondary distribution centered around 5 microns is seen for SWCNT concentrations between 0.04 and 4 µg/cm² which becomes more pronounced with time (see data at 48h in Fig. 6). Regarding time dependence, significant variations from 1 to 24 and 48 hours are seen for 0.04 ng/cm² and for 4 µg/cm² SWCNTs samples.

For both MWCNT and SWCNT data sets, the measured size distributions at low CNT concentrations are similar to the control. This can be due to the fact that at such low concentrations, the CNTs are below the detection limit of the instrument. In addition, some anomalies in the data are likely caused by sedimentation of CNTs during the measurements.

Zeta potential measurements for CNTs in culture media are summarized in Table 1. Compared to the zeta potential of control of -4.7 mV, molecular aggregates in the presence of CNTs are generally more negative reaching -10 mV in some samples. The average zeta potentials ± SEM (n=7) for suspensions of fullerenes,
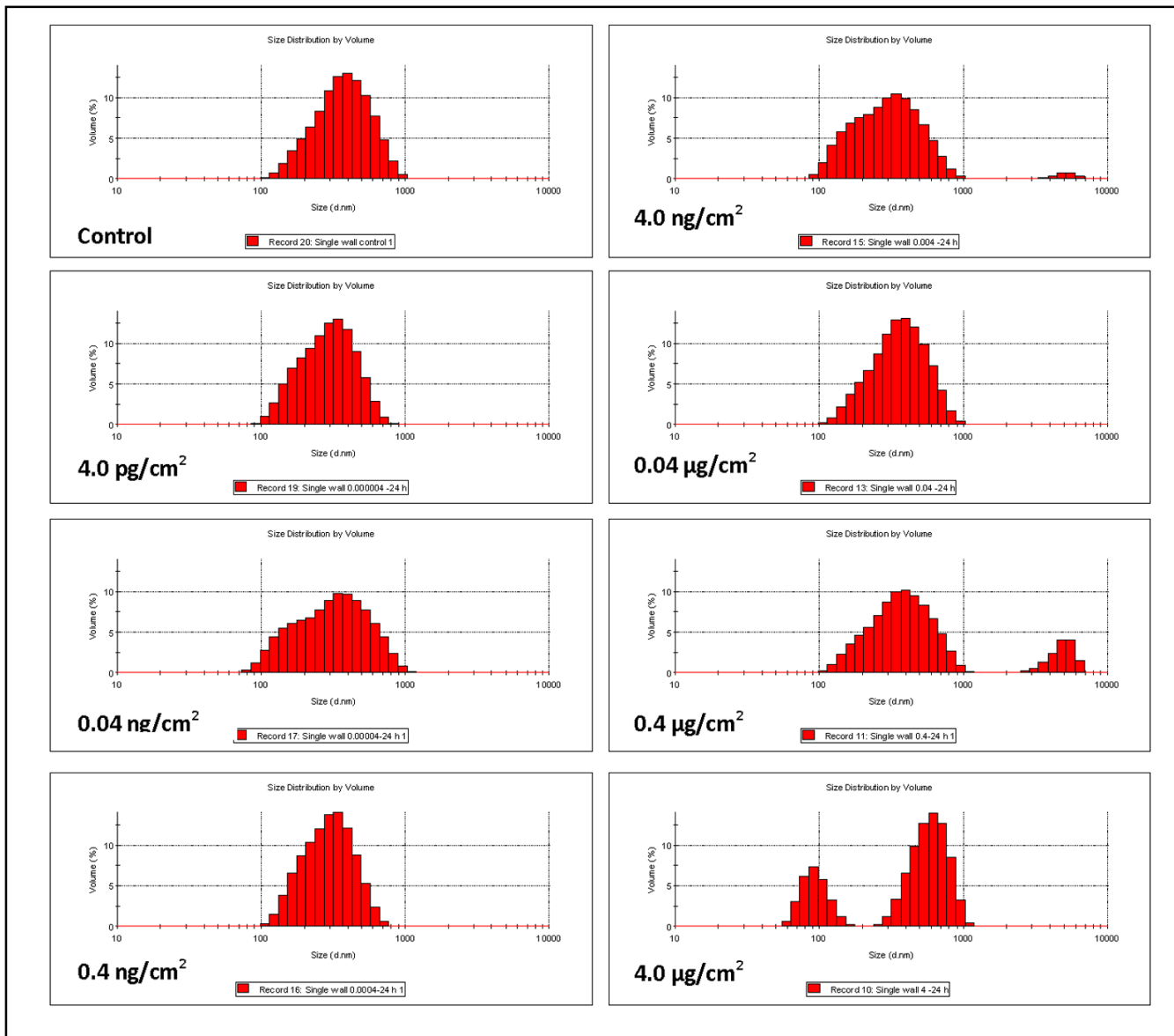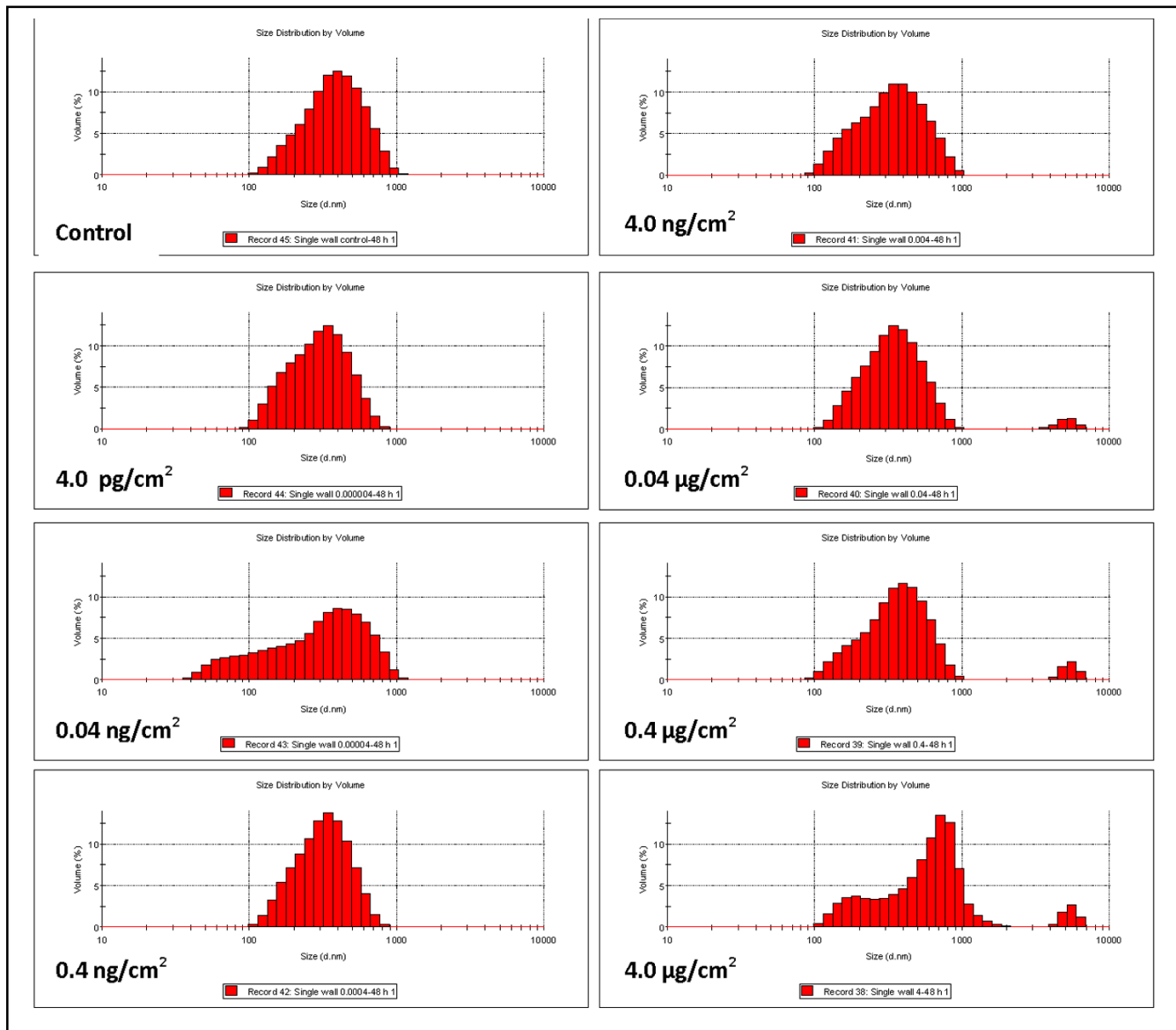
Fig. 5. Particle size measurement of SWCNTs - 24 h incubation. The culture media containing different concentrations (0, 4 μg/cm²-4 pg/cm²) of SWCNTs was prepared in a manner identical to the cell incubation media and incubated at 37 °C for 24 h. The particle sizes were measured by using Zetasizer nano ZS90. The graphs are the original printout from the Zetasizer. The graphs plot size (d.nm) on the x axis versus volume (%) on the Y axis. The top line on each Y axis is 10.

SWCNT and MWCNT in culture media are -8.0 ± 0.6, -7.6 ± 0.7 and -6.1 ± 0.6 mV, respectively. Note that the measured zeta potentials are averages over all molecular aggregates present in the sample which include proteins in the media, CNT aggregates and possible protein-CNT complexes.

Numerous studies have shown that air interface cultures (AIC) simulate *in vivo* conditions more efficiently than the more commonly used liquid covered cultures (LCC) [27-29]. For the Calu-3 cell line, AIC show higher TEER and basal SCC than LCC. In the present study, AIC demonstrated a maximum TEER of 881 Ω.cm² after 14 days which was higher than that demonstrated by LCC (387 Ω.cm²) in the same time period.

Experiments were conducted to determine functional changes induced by exposure of CNPs. To examine the effect of culture exposure time and concentration, Calu-3 cells were grown to confluency and treated with CNPs

Fig. 6. Particle size measurement of SWCNTs - 48 h incubation. The culture media containing different concentrations (0, 4 µg/cm²-4 pg/cm²) of SWCNTs was prepared in a manner identical to the cell incubation media and incubated at 37 °C for 48 h. The graphs are the original printout from the Zetasizer. The graphs plot size (d.nm) on the x axis versus volume (%) on the Y axis. The top line on each Y axis is 10.

for 1, 24 or 48 hours over a concentration range of 4 µg/cm² - 4 pg/cm². For the 1 and 24 time points, the CNPs were added only to the apical bathing media to simulate a more acute exposure. For the 48 hour exposure, the CNPs were added to both the apical and basolateral bathing media. Electrophysiological studies were used to determine the effect of CNPs on TEER, a measure of barrier integrity, and SCC, a measure of hormone responsiveness.

Alterations in TEER after exposure to carbon nanoparticles are shown in Figure 7. All three CNPs were

	C60	SWNT	MWNT
4 µg/cm²	-7.0	-8.9	-3.0
0.4 µg/cm²	-9.2	-8.5	-6.7
0.04 µg/cm²	-9.7	-5.0	-7.2
4 ng/cm²	-8.2	-5.5	-7.0
0.4 ng/cm²	-4.8	-9.9	-4.6
0.04 ng/cm²	-8.0	-6.7	-7.2
4 pg/cm²	-9.1	-8.6	-7.2
control	-4.7		

**Table 1.** Zeta potential (mV) of the CNPs in media.
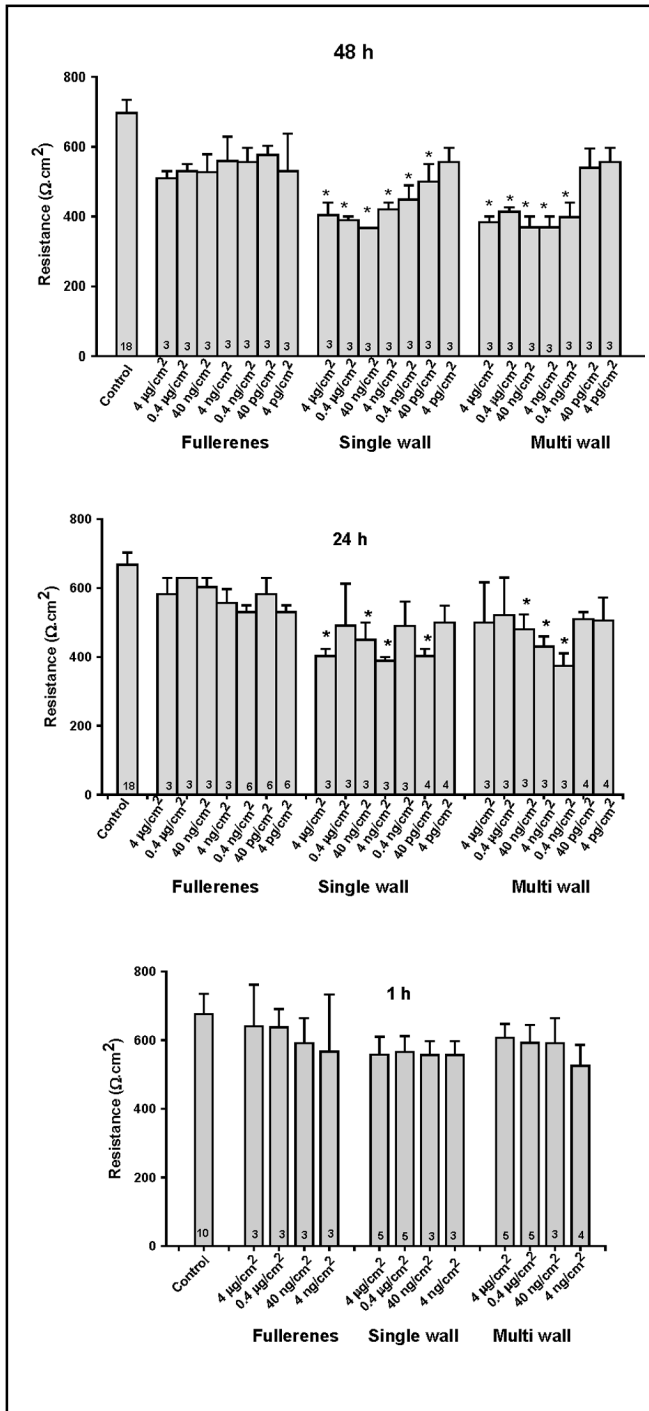
Fig. 7. Effect of 48 h, 24 h and 1 h CNP exposure on TEER of Calu-3 cells. Calu-3 cells were grown for 14 days to form a high resistance monolayer on transwell membrane supports under air interface conditions and treated with CNPs for time periods as indicated in the figure. After the treatment time, the cells were excised from the transwells and mounted in Ussing chambers for measurement of TEER. The number at the base of each bar indicates the number of separate cultures that were measured. Columns indicate means ± SEM. * indicates that the value was statistically different from the control value (P<0.05) using Students' t-test.
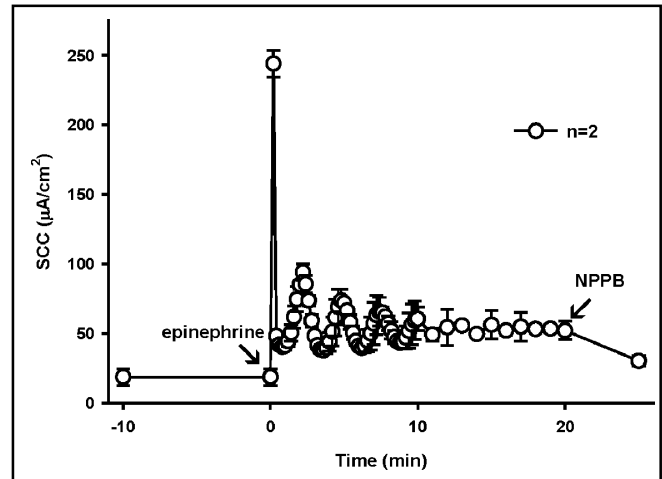

Fig. 8. Response of Calu-3 cells to epinephrine. Confluent monolayers of Calu-3 cells were grown on permeable transwell membranes for 14 days and subsequently mounted in a Ussing chamber where the cells were allowed to develop a stable basal SCC. The graph depicts the measurement of short circuit current (SCC), a measure of net ion transport of the nanoparticle exposed cells. At time=0, epinephrine (10^{-6}M) was added to the serosal bathing medium. At time=20 min, NPPB (100 µM) was added to inhibit the Cl⁻ secretion. The response consisted of several ion transport fluctuations characterized by progressively dampened peaks.

without effect after an hour of exposure. Likewise, no significant reduction in TEER of the monolayer was observed in the case of fullerene exposures at any of the time points or concentrations studied. Conversely, 24 or 48 hours of nanotube (SWCNT and MWCNT) exposure over a wide range of concentrations caused a decrease in TEER. After 48 hours of exposure, the SWCNTs demonstrated effects in the concentration range of 4 µg/cm² to 40 pg/cm² whereas MWCNTs showed the effects in the range of 4 µg/cm² to 0.4 ng/cm². At 24 hrs, the resistance decreases were more variable with the overall effect roughly between the effects seen with 1 h and 48 h exposures. Interestingly, none of these concentrations were toxic to the cells and did not affect the monolayer viability as evidenced by the substantial remaining TEER and absence of any cytokine release. The cytokines measured included TNF-α, IFNr, G-CSF, GM-CSF, IL-1a, IL-8, IP-10 and RANTES. Each of the cytokines was measured in triplicate in each of three separate experiments using the apical and basolateral media of cells exposed to either 4 µg/cm² or 4 ng/cm² of nanotubes. No change in any cytokine release was detected (data not shown).

After placement in the Ussing chambers, the cultures exhibit a stable basal current within 30 minutes. The basal
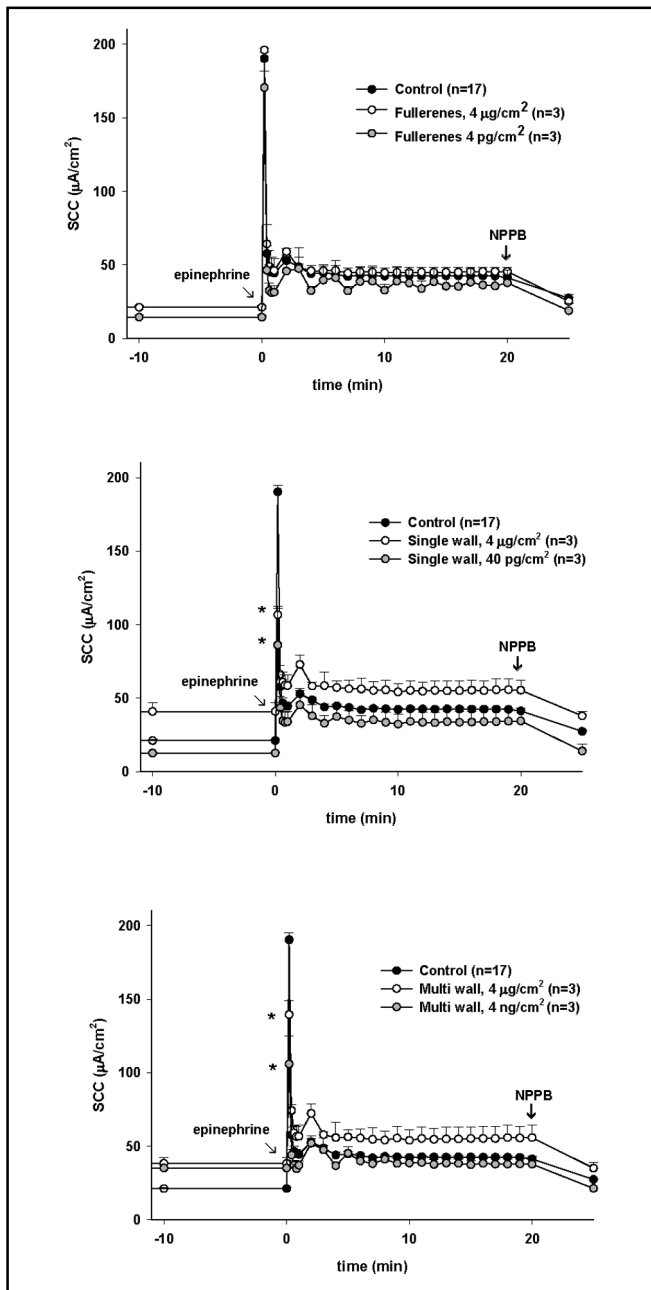
Fig. 9. Epinephrine-stimulated ion transport in the Calu-3 cell line after 48 h nanoparticle incubation. The graphs depict the measurement of SCC, in the control and nanoparticle exposed cells (fullerene, SWCNT and MWCNT respectively from top to bottom). The top figures illustrate the SCC plot of the highest and lowest exposure concentrations of fullerenes for 48 h. The middle and bottom graphs illustrate the responses of the highest and lowest nanotube concentrations that had a significant effect on epinephrine stimulated ion transport. When a stable baseline was achieved, epinephrine (10^{-6}M) was added to the cultures (time t=0). NPPB (100 μM) was added 20 minutes after the epinephrine. The points on the graphs are means + SEM of the number of experiments conducted. * indicates that the value was statistically different from the control value (P<0.05) using Students' t-test.
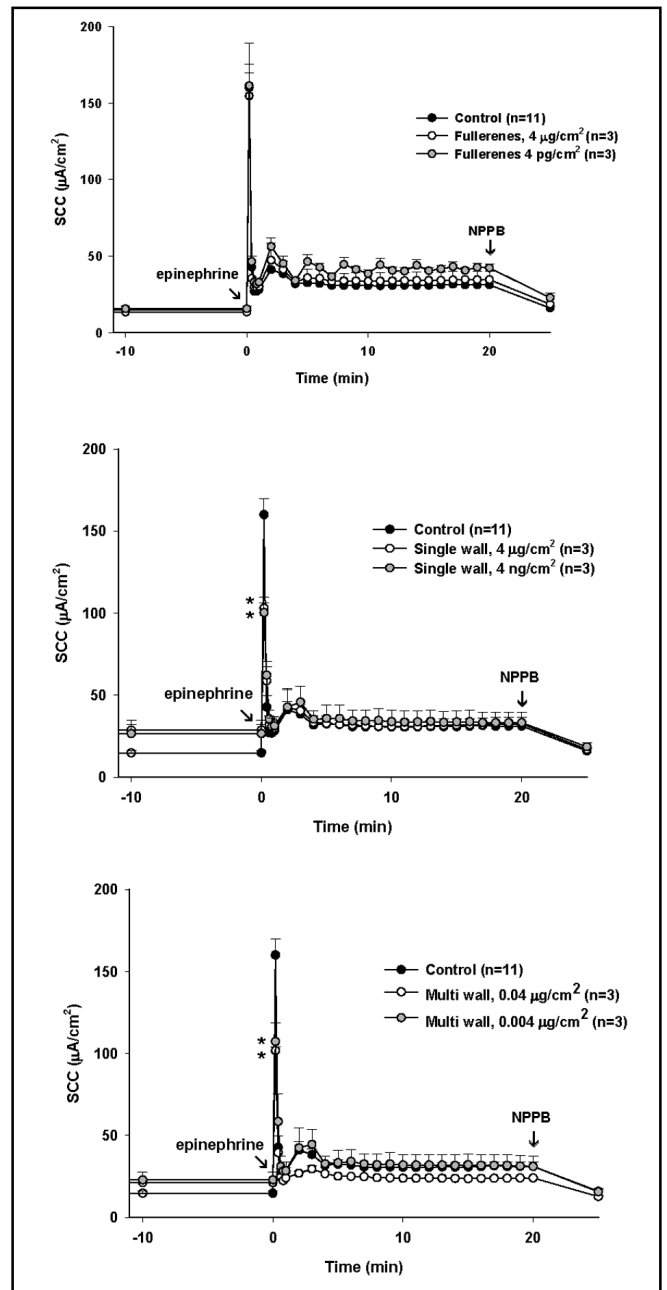
Fig. 10. Epinephrine-stimulated ion transport in the Calu-3 cell line after 24 hour incubation with nanoparticles. The graphs depict the continuous measurement of SCC, in the control and nanoparticle exposed cells (fullerene, SWCNT and MWCNT respectively from top to bottom). The top figures illustrate the SCC plot of the highest and lowest exposure concentrations of fullerenes for 24 h. The middle and bottom graphs illustrate the responses of the highest and lowest nanotube concentrations that had a significant effect on epinephrine stimulated ion transport. When a stable baseline was achieved, epinephrine (10^{-6}M) was added to the cultures (time t=0). NPPB (100 μM) was added 20 minutes after the epinephrine. The points on the graphs are means ± SEM of the number of experiments conducted. * indicates that the value was statistically different from the control value (P<0.05) using Students' t-test.
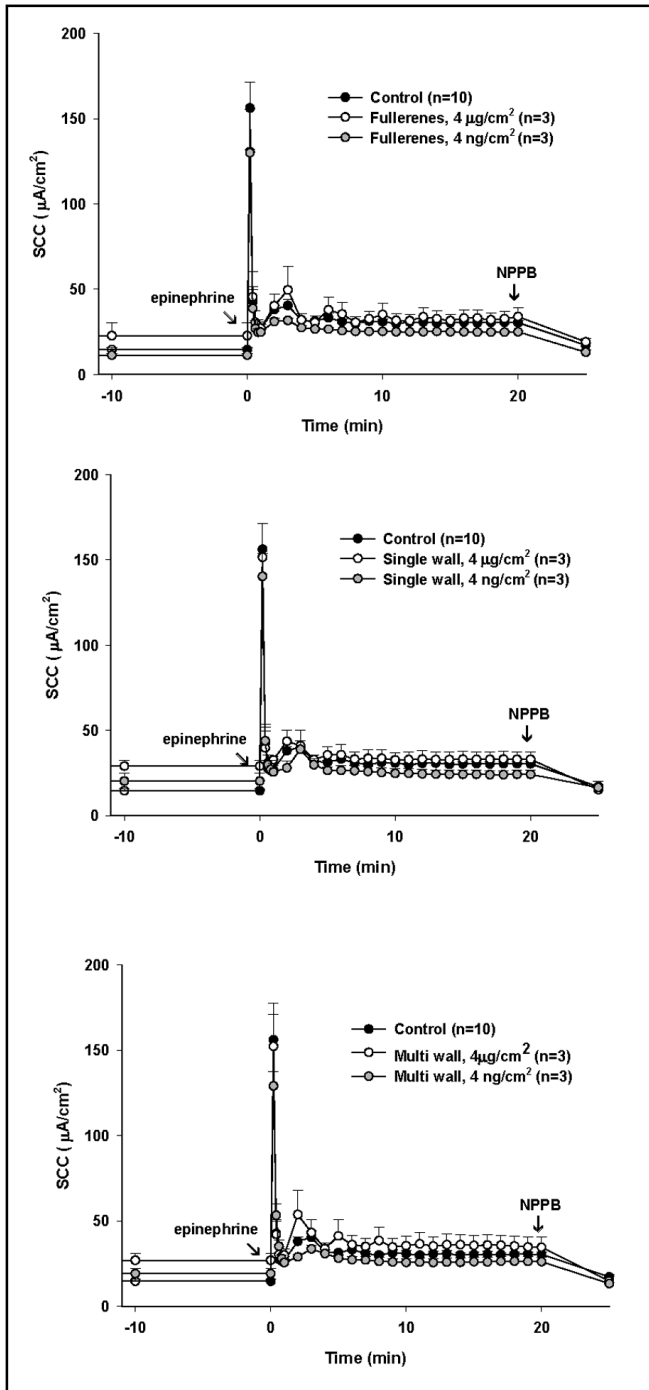
Fig. 11. Epinephrine-stimulated ion transport in the Calu-3 Cell Line after 1 h incubation with nanoparticles. The graphs depict the continuous measurement of SCC, in the control and nanoparticle exposed cells (fullerene, SWCNT and MWCNT respectively from top to bottom). The figures illustrate the SCC plot of the highest and lowest exposure concentrations. When a stable baseline was achieved, epinephrine (10^{-6} M) was added to the cultures (time t=0). NPPB (100 μM) was added 20 minutes after the epinephrine. The points on the graphs are means ± SEM of the number of experiments conducted. None of the treated samples were significantly different than the control using Students' t-test.
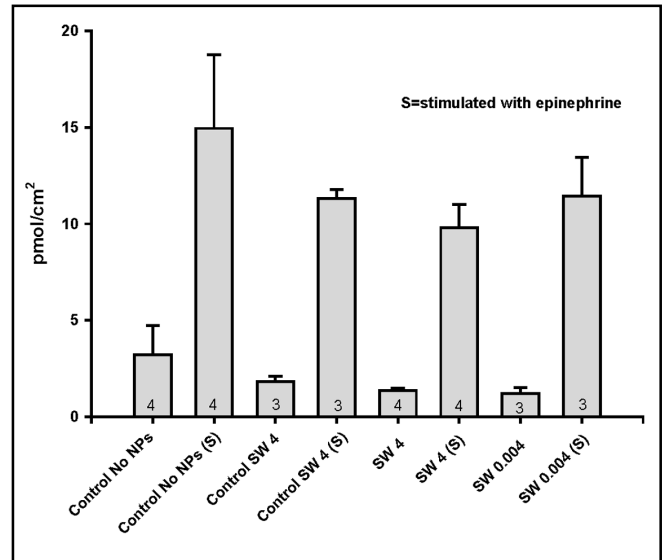
Fig. 12. cAMP concentration in cells treated with SWCNT at a concentration of 4 and 0.004 μg/cm^2 vs untreated cells. The CNPs are known to interfere in the colorimetric assays so a control with CNPs added at the time of experiment was included in addition to a no NP control. The values at the base of the bars represent the number of experiments. The two controls (+/- nanoparticles at the time of experiment) did not differ significantly from each other. Neither of the treated samples had cAMP levels that were significantly different than controls under basal or stimulated conditions.

SCC is due to Cl$^-$ flux in a secretory direction (data not shown). To determine whether the nanoparticles induce changes in cellular function, the response to epinephrine stimulation was studied. Epinephrine is an endogenous hormone that binds α- and β-adrenergic receptors and increases cAMP levels in Calu-3 cells [30]. The stimulation results in an average eight fold increase over the basal ion transport. This cell line has also been shown to exhibit an increase in basal ion transport within 1-2 minutes after exposure to mediators like isoproterenol, forskolin, bradykinin, methacholine, trypsin, histamine [20]. This sudden increase is followed by marked progressively dampening oscillations over time (Fig. 8). We (unpublished data) and others have shown that epinephrine stimulates transepithelial Cl$^-$ transport in a secretory direction (serosal to mucosal) [20, 28, 30]. The first peak represents the most robust response to epinephrine in these cells. For simplicity, only the magnitude of this initial Cl$^-$ secretory response was measured to determine effects of nanoparticles.

The response to epinephrine stimulation after 48, 24 or 1 hour of nanoparticle exposure are shown in Fig. 9-11
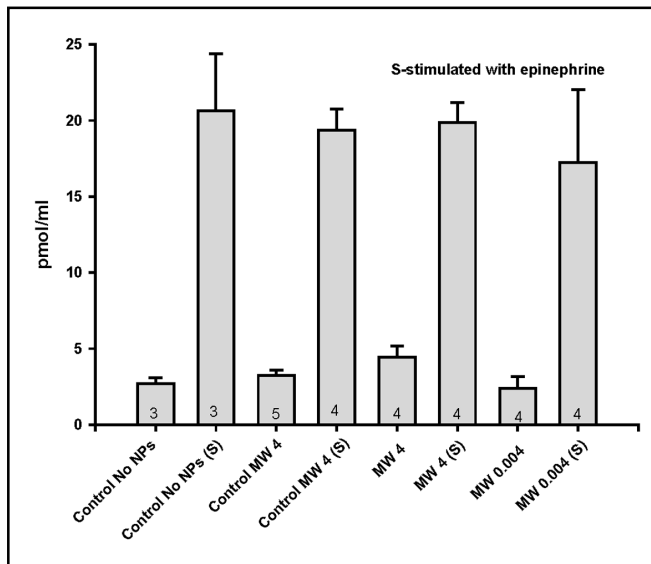
Fig. 13. cAMP concentration in cells treated with MWCNT at a concentration of 4 and 0.004 μg/cm² vs untreated cells. The CNPs are known to interfere in the colorimetric assays so a control with CNPs added at the time of experiment was included in addition to a no NP control. The values at the base of the bars represent the number of experiments. The two controls (+/- nanoparticles at the time of experiment) did not differ significantly from each other. Neither of the treated samples had cAMP levels that were significantly different than controls under basal or stimulated conditions.

respectively. No change in Cl⁻ secretion was observed in response to fullerene exposure. For simplicity, only a high and low fullerene concentration are presented in all figures. However, exposure to either of the nanotubes for 24 or 48 hours caused a decrease in hormone-stimulated Cl⁻ transport over roughly the same concentration range as seen in the TEER measurements. For clarity, only the highest and lowest nanotube concentrations that have significant effects on Cl⁻ secretion are shown. All intermediate concentrations were assayed and exhibited similar patterns (data not shown).

After 1 hour of exposure, there were no nanoparticle-induced changes in epinephrine stimulated Cl⁻ secretion so only the highest and lowest concentrations are depicted although intermediate concentrations were assayed with similar results (Fig. 11).

The initial increase in Cl⁻ secretion is predominately mediated by an increase in intracellular cAMP resulting in activation of PKA and consequently phosphorylation and activation of CFTR. Neither the basal nor the epinephrine stimulated level of cAMP was altered by nanoparticle exposure (Fig. 12-13). These results suggest

that the ion transport element affected by the nanoparticles lies beyond the basolateral membrane epinephrine receptor and intracellular cAMP production.

Discussion

In this study, we have used unpurified, "as manufactured" CNPs to determine potential effects on airway serous epithelial cells. Since these materials form the basis of generation of other types of nanoparticles, their manufacturing process is one of the leading sources of occupational and environmental pollution.

CNPs, particularly nanotubes, are highly hydrophobic and they tend to aggregate into larger complexes [31-33]. Ultrasonic dispersion in a protein-containing solution is the preferred method of increasing solubility and decreasing particle size. However, even this method does not fully solubilize the CNPs. Higher concentrations (μg/cm²) of CNTs will tend to aggregate into larger agglomerates even in the presence of protein.

In our previous publication [26], several methods were used to determine the relative particle sizes of the same CNPs in the media. Results of AFM analysis and dielectric spectroscopy suggested agglomeration at higher concentrations and increased solubilization of CNPs at lower concentrations. The current size measurement provides a relative quantification of particles and agglomerates between 10 nm and 10 μm. This method will not measure agglomerates that are visible to the naked eye such as those detected at our highest concentration of 4 μg/cm². It should be noted that formation of aggregates with sizes above 10 μm will deplete the available CNTs for measurement within the 10 nm to 10 μm range. This explains why the particles variations in the measured range do not show huge variations in amounts despite a 7 order of magnitude difference in concentration. Due to the agglomeration of nanoparticles at higher concentrations and better dispersion at lower concentrations, these particles may exhibit different effects at different levels of exposure. Micro-effects would be due to exposure to agglomerated particles and nano-effects due to exposure to individual particles or small bundles.

Further characterization is provided by the zeta potential measurements of the CNPs in culture media. These measurements were performed across the entire dose range of CNPs. For all samples, the measured zeta potential was negative indicating that the mobile aggregates in the CNP-serum protein solutions have net

negative surface charge. Negative value of the zeta potential suggests that these particles should repel each other electrostatically and agglomeration should be prevented. However, the measured zeta potentials are signficantly smaller than the thermal energy per unit of charge which corresponds to 25 mV at room temperature [34]. Therefore thermal energy alone can overcome the electrostatic barrier. In addition, attractive Van der Waals forces between CNTs and between CNTs and proteins can further contribute to overcoming the repulsive electrostatic forces between these particles. This causes the nanotubes to agglomerate, particularly at higher concentrations where the number of particles per mL of the media is much greater.

We have recently reported that nanoparticles (fullerenes, SWCNT and MWCNT) alter the TEER of a renal cell line model of the principal cells of the distal nephron [26]. In the renal cells, higher concentrations of nanoparticles ($40 \mu g/cm^2$-$0.4 \mu g/cm^2$) were without effect on TEER while lower concentrations ($0.04 \mu g/cm^2$-0.4 ng/cm^2), similar to the levels used in the current study, significantly decreased TEER. Unlike the renal cells that showed no nanoparticle-induced change in hormonal response, the Calu-3 cells exhibit decreases in epinephrine stimulated Cl$^-$ secretion in addition to the changes in barrier properties of the epithelial monolayer.

These results are, in principle, in agreement with previous TEER measurements of Rotoli *et al.* [35] who demonstrated a significant decrease in TEER of Calu-3 monolayers exposed to 100 $\mu g/ml$ of MWCNTs or SWCNTs. The decrease in TEER was also accompanied by an increase in permeability shown by mannitol permeability experiments with no significant alteration in monolayer viability. Our results confirm this work and extend the findings into more physiologically relevant concentrations. For comparison, the highest concentration used in our studies ($4 \mu g/cm^2$) is $100 \mu g/mL$.

While both SWCNT and MWCNT impair the barrier function of Calu-3 monolayers, the change in TEER is not consistent with an altered viability of the cells. The observed changes in resistances indicate subtle changes associated with membrane, cytoskeleton or junctional complexes. Loss of viability in the cellular monolayer would cause a decrease in TEER to unmeasureably low levels. This is also corroborated by cytokine release studies. The absence of cytokine release indicates lack of inflammation or irritation in these cells.

Calu-3 cells express multiple Cl$^-$ channels one of which is CFTR, a channel activated via the adenylyl cyclase/cAMP/PKA pathway [20, 36]. The initial peak in response to epinephrine is cAMP-PKA mediated Cl$^-$ secretion via CFTR channels [30, Blazer-Yost and Banga, unpublished observations]. Many studies, particularly those in the cystic fibrosis field, have demonstrated the importance of Cl$^-$ transport and the accompanying water flux in keeping the viscous secretions of the airways and lungs hydrated. The inhibition of stimulated Cl$^-$ transport during chronic nanotube exposure may have pathological implications resulting from a decreased mucociliary clearance.

The absence of a nanoparticle induced change in cAMP levels after epinephrine stimulation at all the concentrations suggests that at least the initial intracellular signaling pathway is intact. Additional experimentation will be necessary to elucidate the exact site of the CNT effect on both TEER and hormone-stimulated Cl$^-$ transport.

Workplace exposures to nanotubes are difficult to assess. Using currently available methods, different groups have applied different approaches in assessing the workplace levels of nanoparticles [37-40]. For example, Maynard et al. [40] estimated the air borne concentration of nanotubes material generated during handling and suggested that the concentrations were lower than 53 $\mu g/m^3$. Therefore, effects of these nanoparticles in the pg/cm^2 range suggest that workplace levels, particularly during chronic exposures, are likely to have physiological effects that can cause or exacerbate respiratory problems.

Given the potential physiological effects on mucocilliary clearance, it is of interest to correlate the exposure levels of the cultured cells with the aerosolized levels that are likely to occur in the workplace. As a first approximation toward this goal, we have calculated the approximate level of cell exposure to the CNTs. Due to the consistency of effects on both TEER and epinephrine-stimulated Cl$^-$ transport over huge concentration ranges, it is likely these are nanoeffects rather than microeffects. Assuming that the lower concentrations most accurately model the nanoeffects, we have calculated the exposure/ cell if all particles existed as individual nanotubes. The nanotubes used in these experiments have a variable molecular weight because they vary in length from 5-15 μm. Therefore the calculations were performed using molecular weights of the nanoparticles representing both the high and low values. The calculations represent the lowest effective concentrations of 40 pg/cm^2 for the SWCNT and 4 ng/cm^2 for the MWCNTs with an estimation of 1 million cells/cm^2 at confluent density. Under these parameters the estimated exposure levels for the

cultures treated with SWCNT are 0.5-1.4 particles per cell and for the MWCNT was 0.023-0.008 nanoparticles per cell. The latter value can be converted into 1 particle for every 43-132 cells.

Published studies have, for the most part, concentrated on toxic effects of CNTs. However, the current studies suggest that any exposure that allows CNTs to enter the airways may have detrimental effects on normal physiological function, particularly in those individuals with existing respiratory complications such as allergies or asthma.

References

1 Oberdorster G, Oberdorster E, Oberdorster J: Nanotoxicology: An emerging discipline evolving from studies of ultrafine particles. Environ Health Perspect 2005;113:823-839.

2 http://www.nanotechproject.org/inventorie/cnsumer:Woodrow Wilson International Center for Scholars, August 2009.

3 Balbus JM, Maynard AD, Colvin VL, Castranova V, Daston GP, Denison RA, Dreher KL, Goering PL, Goldberg AM, Kulinowski KM, Monteiro-Riviere NA, Oberdorster G, Omenn GS, Pinkerton KE, Ramos KS, Rest KM, Sass JB, Silbergeld EK, Wong BA: Meeting report: Hazard assessment for nanoparticles—report from an interdisciplinary workshop. Environ Health Perspect 2007;115:1654-1659

4 Jia G, Wang H, Yan L, Wang X, Pei R, Yan T, Zhao Y, Guo X: Cytotoxicity of carbon nanomaterials: Single-wall nanotube, multi-wall nanotube, and fullerene. Environ Sci Technol 2005;39:1378-1383.

5 Soto KF, Carrasco A, Powell TG, Garza KM, Murr LE: Comparative in vitro cytotoxicity assessment of some manufactured nanoparticulate materials characterized by transmission electron microscopy. J Nanopart Res 2005;7:145-169.

6 Colvin VL: The potential environmental impact of engineered nanomaterials. Nat Biotechnol 2003;21:1166-1170.

7 Hoet PH, Nemmar A, Nemery B: Health impact of nanomaterials? Nat Biotechnol 2004;22:19.

8 Oberdorster G, Maynard A, Donaldson K, Castranova V, Fitzpatrick J, Ausman K, Carter J, Karn B, Kreyling W, Lai D, Olin S, Monteiro-Riviere N, Warheit D, Yang H: Principles for characterizing the potential human health effects from exposure to nanomaterials: Elements of a screening strategy. Part Fibre Toxicol 2005;2:8.

9 Nel A, Xia T, Madler L, Li N: Toxic potential of materials at the nanolevel. Science 2006;311:622-627.

10 Dhawan A, Taurozzi JS, Pandey AK, Shan W, Miller SM, Hashsham SA, Tarabara VV: Stable colloidal dispersions of C60 fullerenes in water: Evidence for genotoxicity. Environ Sci Technol 2006;40:7394-7401.

11 Donaldson K, Aitken R, Tran L, Stone V, Duffin R, Forrest G, Alexander A: Carbon nanotubes: A review of their properties in relation to pulmonary toxicology and workplace safety. Toxicol Sci 2006;92:5-22.

12 Card JW, Zeldin DC, Bonner JC, Nestmann ER: Pulmonary applications and toxicity of engineered nanoparticles. Am J Physiol Lung Cell Mol Physiol 2008;295:L400-411.

13 Donaldson K, Tran CL: An introduction to the short-term toxicology of respirable industrial fibres. Mutat Res 2004;553:5-9.

14 Mauderly JL, Snipes MB, Barr EB, Belinsky SA, Bond JA, Brooks AL, Chang IY, Cheng YS, Gillett NA, Griffith WC: Pulmonary toxicity of inhaled diesel exhaust and carbon black in chronically exposed rats. Part I: Neoplastic and nonneoplastic lung lesions. Res Rep Health Eff Inst 1994;68:1-75.

15 Lam CW, James JT, McCluskey R, Hunter RL: Pulmonary toxicity of single-wall carbon nanotubes in mice 7 and 90 days after intratracheal instillation. Toxicol Sci 2004;77:126-134.

16 Oberdorster G, Sharp Z, Atudorei V, Elder A, Gelein R, Kreyling W, Cox C: Translocation of inhaled ultrafine particles to the brain. Inhal Toxicol 2004;16:437-445.

17 Kreuter J, Shamenkov D, Petrov V, Ramge P, Cychutek K, Koch-Brandt C, Alyautdin R: Apolipoprotein-mediated transport of nanoparticle-bound drugs across the blood-brain barrier. J Drug Target 2002;10:317-325.

18 Ryman-Rasmussen JP, Cesta MF, Brody AR, Shipley-Phillips JK, Everitt JI, Tewksbury EW, Moss OR, Wong BA, Dodd DE, Andersen ME, Bonner JC: Inhaled carbon nanotubes reach the subpleural tissue in mice. Nat Nanotechnol 2009;4:747-751.

19 Bihari P, Holzer M, Praetner M, Fent J, Lerchenberger M, Reichel CA, Rehberg M, Lakatos S, Krombach F: Single-walled carbon nanotubes activate platelets and accelerate thrombus formation in the microcirculation. Toxicology 2010;269:148-154.

20 Shen BQ, Finkbeiner WE, Wine JJ, Mrsny RJ, Widdicombe JH: Calu-3: A human airway epithelial cell line that shows cAMP-dependent Cl⁻ secretion. Am J Physiol Lung Physiol 1994;266:L493-501.

21 Foster KA, Avery ML, Yazdanian M, Audus KL: Characterization of the Calu-3 cell line as a tool to screen pulmonary drug delivery. Int J Pharm 2000;208:1-11.

22 Buford MC, Hamilton RF Jr, Holian A: A comparison of dispersing media for various engineered carbon nanoparticles. Part Fibre Toxicol 2007;4:6.

23 Vippola M, Falck GC, Lindberg HK, Suhonen S, Vanhala E, Norppa H, Savolainen K, Tossavainen A, Tuomi T: Preparation of nanoparticle dispersions for in-vitro toxicity testing. Hum Exp Toxicol 2009;28:377-385.

24 Guo L, Von Dem Bussche A, Buechner M, Yan A, Kane AB, Hurt RH: Adsorption of essential micronutrients by carbon nanotubes and the implications for nanotoxicity testing. Small 2008;4:721-727.

25 Worle-Knirsch JM, Pulskamp K, Krug HF: Oops they did it again! Carbon nanotubes hoax scientists in viability assays. Nano Lett 2006;6:1261-1268.

26 Blazer-Yost BL, Banga A, Amos A, Chernoff E, Lai X, Li C, Mitra S, Witzmann FA: Effect of carbon nanoparticles on renal epithelial cell structure, barrier function, and protein expression. Nanotoxicology 2011:5:354-371.

27 Grainger CL, Greenwell LL, Lockley DJ, Martin GP, Forbes B: Culture of Calu-3 cells at the air interface provides a representative model of the airway epithelial barrier. Pharm Res 2006;23:1482-1490.

28 Moon S, Singh M, Krouse ME, Wine JJ: Calcium-stimulated Cl⁻ secretion in calu-3 human airway cells requires CFTR. Am J Physiol Lung Physiol 1997;273:L1208-1219.

29 Jeffery PK: Morphologic features of airway surface epithelial cells and glands. Am Rev Respir Dis 1983;128:S14-20.

30 Liedtke CM, Cole TS: Antisense oligonucleotide to PKC-epsilon alters cAMP-dependent stimulation of CFTR in Calu-3 cells. Am J Physiol Cell Physiol 1998;275:C1357-1364.

31 Pauluhn J: Subchronic 13-week inhalation exposure of rats to multiwalled carbon nanotubes: Toxic effects are determined by density of agglomerate structures, not fibrillar structures. Toxicol Sci 2010;113:226-242.

32 Pauluhn J: Multi-walled carbon nanotubes (baytubes): Approach for derivation of occupational exposure limit. Regul Toxicol Pharmacol 2010;57:78-89.

33 L'Azou B, Jorly J, On D, Sellier E, Moisan F, Fleury-Feith J, Cambar J, Brochard P, Ohayon-Courtes C: In vitro effects of nanoparticles on renal cells. Part Fibre Toxicol 2008;5:22.

34 http://physics.nist.gov/cuu/constants/index.html,

35 Rotoli BM, Bussolati O, Bianchi MG, Barilli A, Balasubramanian C, Bellucci S, Bergamaschi E: Non-functionalized multi-walled carbon nanotubes alter the paracellular permeability of human airway epithelial cells. Toxicol Lett 2008;178:95-102.

36 Haws C, Finkbeiner WE, Widdicombe JH, Wine JJ: CFTR in Calu-3 human airway cells: Channel properties and role in cAMP-activated Cl⁻ conductance. Am J Physiol Lung Physiol 1994;266:L502-512.

37 Brouwer D: Exposure to manufactured nanoparticles in different workplaces. Toxicology 2010;269:120-127.

38 Schneider T, Brouwer DH, Koponen IK, Jensen KA, Fransman W, Van Duuren-Stuurman B, Van Tongeren M, Tielemans E: Conceptual model for assessment of inhalation exposure to manufactured nanoparticles. J Expo Sci Environ Epidemiol 2011;21:450-463.

39 Lam CW, James JT, McCluskey R, Arepalli S, Hunter RL: A review of carbon nanotube toxicity and assessment of potential occupational and environmental health risks. Crit Rev Toxicol 2006;36:189-217.

40 Maynard AD, Baron PA, Foley M, Shvedova AA, Kisin ER, Castranova V: Exposure to carbon nanotube material: Aerosol release during the handling of unrefined single-walled carbon nanotube material. J Toxicol Environ Health A 2004;67:87-107.